journal of
thrombosis and haemostasis

Fibrocytes mediate intimal hyperplasia post-vascular injury and are regulated by two tissue factor-dependent mechanisms.

Journal:	*Journal of Thrombosis and Haemostasis*
Manuscript ID:	JTH-2012-01051.R2
Manuscript Type:	Original Article - Vascular Biology
Date Submitted by the Author:	n/a
Complete List of Authors:	Chen, Daxin; King's College London, Dept. of Innate Immunity Ma, Liang; King's College London, Dept. of Innate Immunity Tham, El Li; King's College London, Dept. of Innate Immunity Maresh, Sharnee; King's College London, Dept. of Innate Immunity Lechler, Robert; King's College London, Dept. of Immune Regulation McVey, John; King's College London, Dept. of Innate Immunity Dorling, Anthony; King's College London, Dept. of Innate Immunity
Please select Five Mandatory Key Words from the <a Medical Subject Headings List :	Blood Coagulation, Neointima, Thromboplastin, Vascular System Injuries

Fibrocytes mediate intimal hyperplasia post-vascular injury and are regulated by two tissue factor-dependent mechanisms.

Chen: intimal hyperplasia, TF& fibrocytes.

D. Chen,

L. Ma,

E-L Tham,

S. Maresh,

R. I. Lechler,

J. H. McVey,

A. Dorling.

Medical Research Council (MRC) Centre for Transplantation, King's College London, King's Health Partners, Guy's Hospital, Great Maze Pond, London UK SE1 9RT

Corresponding Author: Prof. Anthony Dorling, MRC Centre for Transplantation, King's College London, Guy's Hospital, London, UK SE1 9RT

Tel +44 (0)20 7188 5880 Fax +44 (0)20 7188 5660

Email; anthony.dorling@kcl.ac.uk

Abstract

Background: $CD34^+$ α-smooth muscle actin $(SMA)^+$ cells mediate intimal hyperplasia (IH) after mechanical endoluminal injury. We previously found that IH is tissue factor (TF) dependent. The precise phenotype of the $CD34^+$ cells mediating IH is unknown and the mechanisms of TF are also unknown.

Objective: To define the phenotype of cells mediating IH and compare the effects of inhibiting (TF) on different subsets of $CD34^+$ cells

Methods: Endoluminal injury was induced in C57BL/6 and two strains of mice expressing a human tissue factor pathway inhibitor (hTFPI) fusion protein on different subsets of $CD34^+$ cells. Confocal microscopy, immunocytofluorescence and real-time PCR were used to determine phenotype.

Results: Neointimal cells in C57BL/6 mice were defined as a subset of fibrocytes ($CD34^+CD45^+$collagen-1^+) expressing SMA, CD31, TIE-2, CXCR4 and CXCL12. Similar cells circulated post-injury and were also found in mice expressing hTFPI on $CD34^+CD31^+$ cells, though in these mice, hTFPI inhibited $CD31^+$ fibrocyte hyperplasia, so no IH developed. Mice with hTFPI on all $CD34^+$ α-SMA^+ cells repaired arteries back to a pre-injured state. No $CD31^+$ fibrocytes were found in these mice unless an anti-hTFPI antibody was administered. Similar findings in protease activated receptor (PAR)-1-deficient mice suggested hTFPI prevented thrombin signalling through PAR-1. In vitro, thrombin increased the number of $CD31^+$ fibrocytes.

Conclusions: Inhibition of TF on $CD31^+$ fibrocytes inhibits IH whereas inhibition on all $CD34^+$ α-SMA^+ cells (or PAR-1 deficiency) inhibits the appearance of $CD31^+$ fibrocytes and promotes repair. These data enhance our understanding of IH and suggest novel ways to promote regenerative repair.

Key words: Blood Coagulation, Neointima, Thromboplastin, Vascular System Injuries.

Introduction

Inflammatory or mechanical injury to blood vessels is followed by a complex response comprising vascular remodeling and intimal hyperplasia (IH) resulting in reduced blood flow and ischaemia of downstream tissues. This type of response is an important cause of blood vessel narrowing in patients with coronary or cerebrovascular disease. Study of IH in murine models [1, 2] has implicated the involvement of coagulation proteins, particularly thrombin, which is generated by a serine protease cascade after exposure of blood to cells expressing tissue factor (TF).

Cells expressing TF are found in the adventitia of blood vessels, where they initiate haemostasis if a vessel is injured. However during an inflammatory response, TF is also expressed by other cell types including leukocytes. In addition to fibrin clot formation, the serine protease cascade generates molecules, including thrombin, that are capable of signalling through protease activated receptors (PAR), of which there are four types, designated PAR 1-4. Thrombin signals through PARs 1,3 and 4 [3]. PAR signalling plays an important role during inflammation [4], and has been shown to influence development of blood vessels including tumour-infiltrating blood vessels [5].

The precise cellular mechanisms through which TF, thrombin and PAR act *in vivo* during IH have hitherto not been characterised. One hypothesis is that they influence smooth muscle cells found in the media of vessels, promoting inflammation, proliferation and migration into the intima. However, significant numbers of intimal α-smooth muscle actin $(SMA)^+$ cells are actually bone marrow (BM)-derived [6, 7] and recent data indicates these are predominantly $CD45^+$ myeloid leukocytes, lacking markers of 'true' SMC [8].

We have previously confirmed this and also shown that these neointimal α–SMA$^+$ cells in C57BL/6 mice (wild-type – WT) have a distinctive phenotype, co-expressing CD45, CD34 and multiple markers classically associated with endothelial cells, including P-selectin, Flk-1, CD31, TIE-2 and E-selectin [9-11], implying a similarity to hemangiocytes or vascular leukocytes, both of which are myeloid lineages involved in angiogenesis, as reviewed recently [12]. Importantly, the cells we described were TF positive.

To demonstrate the importance of TF on these cells, we showed that transgenic mice expressing a membrane-tethered human tissue factor pathway inhibitor (hTFPI) fusion protein ("α–TFPI-Tg" mice) or a hirudin fusion protein on α-SMA$^+$ cells failed to develop neointimal thickening [9]. Although these mice expressed the fusion protein on all medial smooth muscle cells throughout the vasculature, the post-injury phenotype was dependent on expression by bone marrow-derived cells and could be induced in WT mice by transfer of CD34$^+$ cells purified from the circulation of injured Tg mice. After showing that manipulation of CD34$^+$ cells to prevent PAR-1 signalling induced a similar phenotype, we proposed that IH was due entirely to the actions of thrombin (acting through PAR-1), on mobilised CD34$^+$ α-SMA$^+$ cells [10].

Most recently, after allogeneic aortic transplantation, we showed that compared to WT animals, α–TFPI-Tg mice had very different subtypes of circulating CD34$^+$ cells, particularly CD34$^+$α-SMA$^+$ cells. These were predominantly CD45-negative in the Tg mice, whereas in WT they were CD45$^+$ myeloid cells with the phenotype described above [11]. The impact of the hTFPI fusion protein on mobilisation or differentiation of CD34$^+$ subsets was difficult to explain, but our findings were suggested by others to reveal a novel link between bone marrow and blood vessel [13].

In this new work we reverted to a wire-induced endoluminal injury model to explore the mechanisms behind the differences between WT and transgenic animals, and now define the $CD34^+$ α–SMA^+ cells involved in IH and demonstrate two distinct TF-dependent mechanisms acting to regulate both the numbers circulating after injury, and their proliferation after recruitment.

Materials and Methods

An expanded Methods section is available in the Online Data Supplement

Animals and experimental models. WT mice (Harlan Olac Ltd Bicester, UK), heterozygous CD31-TFPI-Tg [14], α-TFPI-Tg [9], homozygous PAR-$1^{-/-}$ (derived from strain B6.129S4-F2rtm1Ajc/J) and PAR-$4^{-/-}$ mice (derived from strain B6.129S4-F2rl3tm1.1Cgh) [15], were bred and maintained at King's College London. All genetically modified animals have been maintained for more than 10 generations on a WT background. All procedures were approved by the UK Home Office. CD31-TFPI-Tg mice have been previously described in detail [14, 16, 17]. These express the hTFPI fusion protein in all $CD31^{+}$ cells including vascular endothelium, platelets and monocytes. However, inclusion of a P-selectin sequence within the cytoplasmic tail means that it is expressed intracellularly in all these cells at rest [18, 19]. We have previously studied these mice in models of LPS endotoxaemia and antibody-mediated rejection, but never in this vascular injury model.

Wire-induced endoluminal carotid artery injury: This was performed as previously described [9, 10]. Briefly, a 100μm diameter wire was introduced and withdrawn three times into the common carotid via the external carotid artery before the external carotid artery was tied off. After confirming restoration of normal blood flow through the common carotid, the skin was closed and animals were allowed to recover.

Morphometric analysis and immunohistology. Sections were prepared and examined as previously described [9, 10]. For analysis of intimal and medial areas, at least three random sections were examined from each of six wire-injured arteries. For immunofluorescence (IF) analysis, consecutive sections were examined either by

a Leica DM-IRBE confocal microscope (Leica, Wetzlar, Germany) and images processed using Leica-TCS-NT software or an IF microscope (Olympus BX51) and analysed with Micro-Manager 1.3 together with Image J software (BioArts, Maryland, USA). For the antibodies used, see the online data supplement.

CD34$^+$ experiments. Purified CD34$^+$ cells were isolated using magnetic beads (Miltentyi Biotech, Surrey UK) as previously described [9, 10] and had an average purity of 95%**.** Flow cytometric analysis was performed on a BD Biosciences LSR Fortessa and data analysed using FlowJo software. For immunocytofluorescence (ICF), at least 300 cells were counted at ×200 magnification from at least 3 random fields from 3 different wells. For functional experiments, CD34$^+$ cells were purified from mice 2-4 days after injury and incubated in vitro with up to 50 nM thrombin (Enzyme Research Laboratories) in Iscove modified Dulbecco medium (Sigma-Aldrich) supplemented with 2% fetal bovine serum (StemCell Technology, Grenoble, France) for 0, 1 or 5 days. A single mouse can provide up to 3 x10^5 CD34+ cells. For adoptive transfer experiments, 1x10^6 CD34$^+$ cells were injected via a tail vein on the day of injury. For RT-PCR analysis, RNA was extracted using the RNAqueous-4PCR kit (Ambion), cDNA made using the SuperScript VILO cDNA Synthesis Kit (Invitrogen), and RT-PCR was performed using Express qPCR SuperMix (Invitrogen) and using TaqMan Gene Expression Assays (Applied Biosystems) on a C100 Thermocycler with a CFX-96 Real-Time PCR Detection Optical Reaction Module (Bio Rad).

Statistical analysis. Data are presented as means ±SEM. Significance of the difference between 2 groups was determined by unpaired Student *t* or log rank test. Values of $P<0.05$ were considered statistically significant.

Results

Neointimal α-SMA$^+$ cells after endoluminal injury are CD34$^+$, CD45$^+$, collagen-1$^+$ fibrocytes expressing CD31.

Wire injury causes loss of endothelium and medial damage, followed by acute inflammation that peaks on day 1, clears by day 7 and is followed by progressive IH [9, 10, 20]. Confocal microscopy of injured WT vessels revealed progressive reappearance of CD31$^+$ cells at the site of injury, which were CD34$^+$, CD45$^+$ and collagen-1$^+$, a constellation of markers consistent with them being fibrocytes. Co-expression of α–SMA is sufficient to label them 'myofibrocytes' (i.e. fibrocytes expressing α-SMA) [21, 22], using terminology in common use, though of course these cells are not from a smooth muscle lineage. The CD31$^+$ myofibrocytes also co-expressed TF, E-selectin and fibronectin (Fig. 1A&B).

In the blood, approximately 50% of circulating CD34$^+$ cells were CD45$^+$ and collagen-1$^+$ (Suppl. Table 1) at the time of peak mobilization (2-3 days post-injury [10]). Double staining of purified CD34$^+$ cells with CD45 and collagen-1 confirmed all collagen-1$^+$ cells were CD45$^+$ consistent with them being fibrocytes (data not shown). 8% of the CD34$^+$ cells were α–SMA$^+$ and of these (Table 1), most were CD90$^+$, CXCL12$^+$ and CXCR4$^+$and expressed CD45, Ly6-C, CD11b, CD115, F4/80, collagen-1 and fibronectin, consistent with most having a myofibrocyte phenotype. Most also expressed TIE-2 and approximately 30% co-expressed CD31 and Flk-1 consistent with the phenotype of the neointimal cells. Thus, CD45$^+$ collagen-1$^+$ α-SMA$^+$ CD31$^+$ myofibrocytes accounted for approximately 3% of circulating CD34$^+$ cells 3 days post-injury (Table 2). The circulating CD34$^+$α-SMA$^+$ CD45$^+$ myeloid cells previously described after allogeneic aortic transplantation [11] were also collagen-1$^+$ (Suppl Table 2).

Response to injury in a strain of Tg mice expressing hTFPI on CD31$^+$ fibrocytes alone.

Analysis of hTFPI fusion protein expression by circulating leukocytes in CD31-TFPI-Tg mice 3 days post-wire-induced injury revealed cell surface expression on 1-2% of CD34$^+$ all of which were CD45$^+$ (Fig. 2A&B). No expression was seen on the surface of CD34-negative cells.

Conventional immunocytofluorescence analysis showed hTFPI in 53 (±4)% of CD34$^+$ cells that were CD31$^+$ (Fig. 2C), but repeat analysis with anti-hTFPI mAb applied *before* permeabilisation showed that cell membrane hTFPI was expressed by only 5% of the CD31$^+$ CD34$^+$ cells (Fig. 2D), all of which were α–SMA$^+$ (illustrated in Fig. 2E) and of these, 84 (±16)% were collagen-1$^+$ and 53 (±17)% fibronectin$^+$. Therefore, cell surface hTFPI in these mice was found exclusively on CD31$^+$ myofibrocytes and was confined intracellularly in all other circulating cells, consistent with intracellular secretory granule localisation in these cells as previously defined [18, 19].

Examination of circulating CD34$^+$ cells and specifically the α–SMA$^+$ CD34$^+$ subset in these mice revealed few significant differences compared to WT (Suppl Table 1, Table 1), except that CD31-TFPI-Tg mice had fewer E-selectin$^+$, and fewer F4/80$^+$ α-SMA$^+$ double positive cells. Nevertheless, they had similar proportions of fibrocytes, myofibrocytes and CD31$^+$ myofibrocytes as WT mice (Table 2). Administration of an anti-hTFPI antibody had no significant influence on the proportions of most of these subsets of CD34$^+$ cells (Table 1,2, suppl table 1), though did increase the proportion of CD34$^+$ α-SMA$^+$ cells expressing angiopoietin-2.

CD31$^+$ myofibrocytes expressing hTFPI were recruited to the intima after wire-induced injury (Fig. 1C&D). But in contrast to WT mice, these mice did not develop

progressive IH at day 28 and the neointima consisted of a single cell layer of myofibrocytes (Fig. 1D). The lack of IH was due to the hTFPI, as administration of an inhibitory anti-hTFPI Ab caused hyperplasia (Fig 2F). Adoptive transfer of $CD34^+$ cells from these mice to injured WT confirmed that Tg $CD34^+$ cells inhibited the development of IH (Fig. 2G). When performed in the reverse direction, WT CD34+ cells caused Tg mice to develop IH, though the lesions were not as profound as those seen in WT animals (Fig 2G).

$CD34^+$ cells in α-TFPI-Tg mice, a strain in which endoluminal injury is followed by regenerative repair.

We did further experiments in a different strain of mice (α-TFPI-Tg mice), which responds to vascular injury by regenerating endothelium without IH [9-11]. As expected in these mice, newly recruited $CD31^+$ cells were $CD34^+$ but negative for α–SMA, CD45, TF, E-selectin and collagen-1 (Fig. 3A&B). This phenotype was hTFPI-dependent, as an inhibitory anti-hTFPI antibody given at the time of injury led to recruitment of $CD31^+$ myofibrocytes (Fig 3C&D). To study recruitment of α-SMA^+ cells, α–TFPI-Tg $CD34^+$ cells were adoptively transferred into injured WT mice, as previously reported [9]. Transferred $CD34^+$α-SMA^+ cells expressing hTFPI were visible by day 3 (Fig. 3E&F). In these analyses, for methodological reasons, vWF rather than CD31 was used as the marker for endothelial antigens; vWF^+ cells were first visible between days 5-7, luminal to areas of hTFPI-expression and distinct from areas of $CD45^+$ staining. By day 28 a new endothelium was visible sitting on a layer of $hTFPI^+$ cells.

Single stain immunocytofluorescence analysis of the circulating $CD34^+$ cells in these mice suggested that the proportion of fibrocytes ($CD34^+$ $CD45^+$ collagen-1^+) was

similar as in WT (Suppl. Table 3). However double staining revealed significant differences in the phenotype of $CD34^+$ α–SMA^+ cells, (Table 3), the majority of which expressed NG2 and CD140b, consistent with a pericyte lineage and there were few collagen-1^+ cells and no $CD31^+$ cells (Table 2). All these differences were hTFPI-dependent (Fig 3G, Table 3).

Flow cytometry showed that cell surface hTFPI was expressed by 3-5% of $CD34^+$ (but not CD34-) cells (Fig. 4 A&B). By conventional immunocytofluorescence, it was found in all α–SMA^+ cells, including $CD45^+$ and $CD45^-$ subsets (Fig 4C-H). Repeat analysis with anti-hTFPI mAb applied *before* permeabilisation showed that only 60% had cell membrane hTFPI, none of which co-expressed CD45, collagen-1 or fibronectin, but all were $NG2^+$ (Fig 4) and 55% were $CD140b^+$. Thus, cell surface hTFPI fusion protein was expressed exclusively by the population of $CD34^+CD45^-$ negative α-SMA^+ cells but was confined intracellularly in the small number of myofibrocytes present.

Based on the assumption that only cell-surface hTFPI has biological function, all this data suggests that the profound changes in the subsets of $CD34^+\alpha$–SMA^+cells circulating after injury, along with the repair phenotype, is due to expression of the hTFPI fusion protein by $CD34^+NG2^+$ cells.

Real-time PCR analysis of collagen-1 expression.

Real time PCR analysis of $CD34^-$ and $CD34^+$ fractions from blood mononuclear cells of all three strains of mice confirmed that collagen-1 was expressed only by $CD34^+$ cells (Fig 4I). Moreover, there was a close correlation between collagen-1 expression (normalised to TBP) by $CD34^+\alpha$-SMA^+ cells and the proportion of $CD34^+\alpha$-SMA^+ cells expressing collagen-1 by immunocytofluorescence (Fig. 4I&J).

Importance of PAR-1 for the presence of the myofibrocytes expressing CD31.

A PAR-1 antagonist administered on the day of injury significantly reduced the $CD31^+$ myofibrocytes in WT mice (Fig. 4K) and PAR-$1^{-/-}$ animals had none of these cells detectable after injury, in contrast to PAR-$4^{-/-}$ mice (Fig. 4K). Instead, $CD34^+$ α–SMA^+ cells in PAR-$1^{-/-}$ mice were mostly CD45- and collagen-1-negative (Suppl. Table 4). Additionally, in vitro incubation of $CD34^+$ cells with thrombin [10] promoted the outgrowth of $CD31^+\alpha$–SMA^+ cells from PAR-$4^{-/-}$ but not PAR-$1^{-/-}$ mice (Fig. 4L&M and Table 8). All this indicates that PAR-1 is required for $CD31^+$ myofibrocytes to appear in the circulation.

$CD31^+$ myofibrocytes also outgrew from thrombin-incubated α–TFPI-Tg $CD34^+$ cells (Fig. 4N-P, Suppl. Table 5), but not when $hTFPI^+$ cells were depleted, or when α–SMA^+ cells were absent naturally, as when taken from sham-injured mice. These data indicate that thrombin-mediated outgrowth of $CD31^+$ myofibrocytes in vitro involves a direct effect of thrombin on an hTFPI-expressing $CD34^+\alpha$-SMA^+ cell.

Discussion

Although the clinical relevance of the wire-induced injury model is debated, it is a well-characterised model of endothelial and medial damage in which the response to injury has been studied in detail, with strengths and weaknesses when it comes to interpreting how data relates to human pathology. Our novel contributions in this paper are to define as fibrocytes the α-SMA$^+$ cells accumulating in neointimal hyperplasia and define two TF-dependent mechanisms regulating their behaviour. The term 'fibrocyte' is old, but cells with a phenotype now called fibrocytes (myeloid cells expressing CD34 and collagen-1) were first described in a mouse wound-healing model [23]. Subsequently, α-SMA expression in cells outgrown from human mononuclear cells (called 'myofibrocytes') has been defined, particularly after incubation with TGF-β1 [24]. The role of fibrocytes in inflammation is still not clear, though they have been linked to chronic inflammatory diseases in humans [22]. In experimental models, myofibrocytes have been associated with IH in sheep [25] and rats [26]. The function of fibrocytes expressing CD31 [21] have not been defined. Compared to previous descriptions, the phenotype of the myofibrocytes described here is atypical and is reminiscent of TIE-2 expressing monocytes or vascular leukocytes [12]. Although consistent with the remarkable plasticity shown by these lineages, this is the first description of this particular constellation of markers on myeloid cells. Consistent with the data indicating the importance of CXCL12/CXCR4 interactions for the development of IH [27], the CD31$^+$ myofibrocytes in this model appeared capable of responding to, and perhaps maintaining CXCL12 chemokine gradients.

The cells accumulating in the neointima of WT mice accounted for ≤ 0.05% of cells found in peripheral blood, a frequency that made characterisation of the cells by flow

cytometry impractical. The immunocytofluorescence technique we employed is time consuming, labour intensive and does not allow comparison of expression levels. However, it is highly suited to analysis of small numbers of cells, reliably assesses protein expression and is easy to interpret. Our interpretation of the immunocytofluorescence data was corroborated by RT-PCR data from all three strains.

With reference to the aims of this study, an important insight into the importance of TF came from CD31-TFPI-Tg mice, which did not develop IH. When $CD34^+$ cells from these mice were adoptively transferred into WT mice, there was significant inhibition of IH, to the extent seen in Tg mice. Having confirmed again in experiments reported here that adoptively transferred $CD34^+$ cells are recruited to the site of injury and considering that cell-membrane expressed hTFPI fusion protein was found only on $CD31^+$ myofibrocytes, we propose that the primary action of hTFPI in these mice was to prevent $CD31^+$ myofibrocytes, from undergoing hyperplasia at the site of injury. This would be compatible with the immunohistological analysis of vessels in CD31-TFPI-Tg mice, which showed a single layer of luminal $CD31^+$ myofibrocytes for up to 28 days post-injury. If correct, the clear implication is that hyperplasia of recruited myofibrocytes is TF-dependent. Our assumption that only cell-surface hTFPI had biological activity is logical. However, we cannot exclude a role for the intracellular hTFPI present in other circulating cells, nor exclude the possibility that TFPI expressed by endothelial cells played a role in the phenotype of these mice, particularly since CD31-TFPI-Tg mice administered WT $CD34^+$ cells developed IH that was less severe than WT mice.

In contrast to the situation in CD31-TFPI-Tg mice, expression of hTFPI under an α–SMA promoter had a profound influence on the sub-types of $CD34^+\alpha$–SMA^+ cells

circulating after injury, suppressing the number of myofibrocytes ($CD34^+$ α-SMA^+ collagen-1^+), particularly those expressing CD31. Instead, $CD34^+$ CD45-negative $NG2^+$ α-SMA^+ cells emerged in the circulation and in these mice, appeared to be the only cells with the hTFPI fusion protein on their cell surface. Our data do not directly address the mechanism by which hTFPI expression in α-SMA^+ cells causes these cells to appear in α-TFPI-Tg mice. However, the data presented here strongly suggest that inhibition of thrombin generation and subsequent signaling through PAR-1 on $CD34^+$ cells is sufficient to explain the absence of $CD31^+$ myofibrocytes. We are currently investigating whether hTFPI-dependent changes in expression of factors such as angiopoietins by $CD34^+$ cells (some of which are illustrated in tables 1 and 3), are important.

In this work, we have not directly assessed whether medial smooth muscle cells (which are obviously α-SMA^+ $hTFPI^+$ in α-TFPI-Tg mice) are involved in vessel repair. However, we have previously shown that the phenotype of α-TFPI-Tg mice is dependent on fusion protein expression by bone marrow-derived cells [9], suggesting no role for medial smooth muscles cells. In addition, adoptive cell transfer experiments indicated that $CD34^+$ cells from these mice, injected into WT mice were recruited to the vessel wall and that transfer of Tg $CD34^+$ cells was sufficient to induce regeneration of a quiescent endothelium. We therefore conclude that re-endothelialisation at the site of injury in α-TFPI-Tg mice occurs because of the presence of the $CD34^+$ CD45-negative $NG2^+$ α-SMA^+ cells in the circulation.

NG2 and α-SMA are expressed by pericytes. Whilst classical pericytes (defined by their location within the vascular basement membrane) are $CD34^-$, $CD34^+$ cells with a pericyte-like phenotype have been defined [28]. Other accepted phenotypic markers include CD140b, desmin and CD13 [29], though there is heterogeneity of expression

of these between different vascular beds and at different stages of maturity, so the cells in α-TFPI-Tg mice could be from a pericyte lineage.

There is some evidence linking pericytes to fibrosis. Humphreys et al, working in a renal model, suggested that pericytes were myofibrocyte / blast precursors [30], consistent with more recent data indicating pro-inflamatory myofibroblasts in skin or skeletal muscle wounds derive from ADAM12$^+$ pericytes [31]. Our data from α-TFPI-Tg mice are compatible with these, because thrombin-dependent outgrowth of CD31$^+$ myofibrocytes from α-TFPI-Tg mice was dependent on the presence of the hTFPI$^+$ population, and we found cell membrane expressed hTFPI only on NG2$^+$ cells. However, the data are also compatible with a more complex relationship between the two cell types, involving thrombin-dependent production of pericyte-derived factors that promote myofibrocyte development.

In summary, we have identified a previously undefined population of CD31$^+$ myofibrocytes in the circulation post-vascular injury, shown that these are the cells recruited to the neointima, implicated TF on these cells as the major stimulus driving their hyperplasia and identified an equilibrium between circulating pericytes and myofibrocytes, maintained by TF and thrombin. These findings help explain the mechanistic link between TF/thrombin and the cellular response to endoluminal injury, redefine our understanding of vascular remodelling in these mouse models and may have significant implications for understanding human IH and promoting regenerative repair.

Acknowledgements

This work was funded by the Medical Research Council UK (Award G0801965). We acknowledge additional financial support from the Department of Health via the National Institute for Health Research (NIHR) comprehensive Biomedical Research Centre award to Guy's & St Thomas' NHS Foundation Trust in partnership with King's College London and King's College Hospital NHS Foundation Trust. We also acknowledge support from the MRC Centre for Transplantation

References

1 Huynh TT, Davies MG, Thompson MA, Ezekowitz MD, Hagen P, Annex BH. Local treatment with recombinant tissue factor pathway inhibitor reduces the development of intimal hyperplasia in experimental vein grafts. *J Vasc Surg*. 2001; **33**: 400-7.

2 Rade JJ, Schulick AH, Virmani R, Dichek DA. Local adenoviral-mediated expression of recombinant hirudin reduces neointima formation after arterial injury. *Nat Med*. 1996; **2**: 293-8.

3 Coughlin SR. Thrombin signalling and protease-activated receptors. *Nature*. 2000; **407**: 258-64.

4 Ma L, Dorling A. The roles of thrombin and protease-activated receptors in inflammation. *Semin Immunopathol*. 2012; **34**: 63-72.

5 Carmeliet P. Biomedicine. Clotting factors build blood vessels. *Science*. 2001; **293**: 1602-4.

6 Shimizu K, Sugiyama S, Aikawa M, Fukumoto Y, Rabkin E, Libby P, Mitchell RN. Host bone-marrow cells are a source of donor intimal smooth- muscle-like cells in murine aortic transplant arteriopathy. *Nat Med*. 2001; **7**: 738-41.

7 Caplice NM, Bunch TJ, Stalboerger PG, Wang S, Simper D, Miller DV, Russell SJ, Litzow MR, Edwards WD. Smooth muscle cells in human coronary atherosclerosis can originate from cells administered at marrow transplantation. *Proc Natl Acad Sci U S A*. 2003; **100**: 4754-9.

8 Iwata H, Manabe I, Fujiu K, Yamamoto T, Takeda N, Eguchi K, Furuya A, Kuro-o M, Sata M, Nagai R. Bone marrow-derived cells contribute to vascular

inflammation but do not differentiate into smooth muscle cell lineages. *Circulation*. 2010; **122**: 2048-57.

9 Chen D, Weber M, Shiels PG, Dong R, Webster Z, McVey JH, Kemball-Cook G, Tuddenham EG, Lechler RI, Dorling A. Postinjury vascular intimal hyperplasia in mice is completely inhibited by CD34+ bone marrow-derived progenitor cells expressing membrane-tethered anticoagulant fusion proteins. *J Thromb Haemost*. 2006; **4**: 2191-8.

10 Chen D, Abrahams JM, Smith LM, McVey JH, Lechler RI, Dorling A. Regenerative repair after endoluminal injury in mice with specific antagonism of protease activated receptors on CD34+ vascular progenitors. *Blood*. 2008; **111**: 4155-64.

11 Chen D, Shrivastava S, Ma L, Tham el L, Abrahams J, Coe JD, Scott D, Lechler RI, McVey JH, Dorling A. Inhibition of thrombin receptor signaling on alpha-smooth muscle actin(+) CD34(+) progenitors leads to repair after murine immune vascular injury. *Arterioscler Thromb Vasc Biol*. 2012; **32**: 42-9.

12 Coffelt SB, Lewis CE, Naldini L, Brown JM, Ferrara N, De Palma M. Elusive identities and overlapping phenotypes of proangiogenic myeloid cells in tumors. *Am J Pathol*. 2010; **176**: 1564-76.

13 Delacroix S, Simari RD. Tissue factor-thrombin-PAR-1 pathway: a novel link between bone marrow and blood vessel. *Arterioscler Thromb Vasc Biol*. 2012; **32**: 3-4.

14 Chen D, Giannopoulos K, Shiels PG, Webster Z, McVey JH, Kemball-Cook G, Tuddenham E, Moore M, Lechler R, Dorling A. Inhibition of intravascular thrombosis in murine endotoxemia by targeted expression of hirudin and tissue factor pathway inhibitor analogs to activated endothelium. *Blood*. 2004; **104**: 1344-9.

15 Connolly AJ, Ishihara H, Kahn ML, Farese RV, Jr., Coughlin SR. Role of the thrombin receptor in development and evidence for a second receptor. *Nature*. 1996; **381**: 516-9.

16 Chen DX, Weber M, McVey JH, Kemball-Cook G, Tuddenham EGD, Lechler RI, Dorling A. Complete inhibition of acute humoral rejection using regulated expression of membrane-tethered anticoagulants on xenograft endothelium. *American Journal of Transplantation*. 2004; **4**: 1958-63.

17 Chen D, Carpenter A, Abrahams J, Chambers RC, Lechler RI, McVey JH, Dorling A. Protease-activated receptor 1 activation is necessary for monocyte chemoattractant protein 1-dependent leukocyte recruitment in vivo. *J Exp Med*. 2008; **205**: 1739-46.

18 Chen D, Riesbeck K, McVey JH, Kemball-Cook G, Tuddenham EG, Lechler RI, Dorling A. Regulated inhibition of coagulation by porcine endothelial cells expressing P-selectin-tagged hirudin and TFPI fusion proteins. *Transplantation*. 1999; **68**: 832-9.

19 Riesbeck K, Chen D, Kemball-Cook G, McVey JH, George AJ, Tuddenham EG, Dorling A, Lechler RI. Expression of hirudin fusion proteins in mammalian cells: a strategy for prevention of intravascular thrombosis. *Circulation*. 1998; **98**: 2744-52.

20 Lindner V, Fingerle J, Reidy MA. Mouse model of arterial injury. *Circ Res*. 1993; **73**: 792-6.

21 Pilling D, Fan T, Huang D, Kaul B, Gomer RH. Identification of markers that distinguish monocyte-derived fibrocytes from monocytes, macrophages, and fibroblasts. *PLoS One*. 2009; **4**: e7475.

22 Reilkoff RA, Bucala R, Herzog EL. Fibrocytes: emerging effector cells in chronic inflammation. *Nat Rev Immunol*. 2011; **11**: 427-35.

23 Bucala R, Spiegel LA, Chesney J, Hogan M, Cerami A. Circulating fibrocytes define a new leukocyte subpopulation that mediates tissue repair. *Mol Med*. 1994; **1**: 71-81.

24 Abe R, Donnelly SC, Peng T, Bucala R, Metz CN. Peripheral blood fibrocytes: differentiation pathway and migration to wound sites. *J Immunol*. 2001; **166**: 7556-62.

25 Varcoe RL, Mikhail M, Guiffre AK, Pennings G, Vicaretti M, Hawthorne WJ, Fletcher JP, Medbury HJ. The role of the fibrocyte in intimal hyperplasia. *J Thromb Haemost*. 2006; **4**: 1125-33.

26 Onuta G, van Ark J, Rienstra H, Boer MW, Klatter FA, Bruggeman CA, Zeebregts CJ, Rozing J, Hillebrands JL. Development of transplant vasculopathy in aortic allografts correlates with neointimal smooth muscle cell proliferative capacity and fibrocyte frequency. *Atherosclerosis*. 2010; **209**: 393-402.

27 Zernecke A, Schober A, Bot I, von Hundelshausen P, Liehn EA, Mopps B, Mericskay M, Gierschik P, Biessen EA, Weber C. SDF-1alpha/CXCR4 axis is instrumental in neointimal hyperplasia and recruitment of smooth muscle progenitor cells. *Circ Res*. 2005; **96**: 784-91.

28 Tallone T, Realini C, Bohmler A, Kornfeld C, Vassalli G, Moccetti T, Bardelli S, Soldati G. Adult human adipose tissue contains several types of multipotent cells. *Journal of cardiovascular translational research*. 2011; **4**: 200-10.

29 Armulik A, Genove G, Betsholtz C. Pericytes: developmental, physiological, and pathological perspectives, problems, and promises. *Dev Cell*. 2011; **21**: 193-215.

30 Humphreys BD, Lin SL, Kobayashi A, Hudson TE, Nowlin BT, Bonventre JV, Valerius MT, McMahon AP, Duffield JS. Fate tracing reveals the pericyte and not epithelial origin of myofibroblasts in kidney fibrosis. *Am J Pathol*. 2010; **176**: 85-97.

31 Dulauroy S, Di Carlo SE, Langa F, Eberl G, Peduto L. Lineage tracing and genetic ablation of ADAM12(+) perivascular cells identify a major source of profibrotic cells during acute tissue injury. *Nat Med*. 2012.

Table 1: Double stain immunocytofluorescence analysis of $CD34^+$ α-SMA^+ cells

	$CD34^+\alpha$-SMA^+ cells – Isolated day 3 post-injury				
	% (±SEM) of $CD34^+\alpha$-SMA^+ cells expressing these ligands				
	WT	CD31-TFPI-Tg	p value	CD31-TFPI-Tg + anti-hTFPI	p value†
CD90	100	100	NS	ND	-
Collagen-1	91.9 (±4)	74.6 (±9.5)	NS	ND	-
Fibronectin	65.8 (±6)	58.6 (±6)	NS	ND	-
Flk-1	42.6 (±10)	30.7 (±8.3)	NS	ND	-
CD31	35.8 (±8.7)	32.4 (±8.8)	NS	37.4 (±10.4)	NS
CD45	54.4 (±18)	51.2 (±12)	NS	ND	-
F4/80	57 (±1.8)	32.6 (±3.9)	0.005	ND	-
Ly6-C	57.4 (±6.3)	55.7 (±11)	NS	ND	-
CD11b	68.3 (±9.3)	53.7 (±2)	NS	ND	-
CD115	56.7 (±14)	46.7 (±6.7)	NS	ND	-
TIE-2	59.1 (±14)	66.2 (±16)	NS	72.3 (±6.4)	NS
CD140b	0	3.7 (±3.7)	NS	ND	-
NG2	0	7.7 (±4.4)	NS	ND	-
Angiopoietin-1	47.9 (±2.1)	42.1 (±4.8)	NS	61.4 (±7.8)	NS
Angiopoietin-2	37.9 (±2.8)	32.2 (±6.1)	NS	70.9 (±6.8)	0.01
CXCL12	97.4 (±2.6)	69.6 (±16.1)	NS	79.6 (±4.6)	NS
CXCR4	93.3 (±6.7)	61.5 (±14.3)	NS	78.3 (±6)	NS

† CD31-TFPI-Tg + anti-hTFPI vs. CD31-TFPI-Tg

ND not done

Table shows proportion of $CD34^+$ α-SMA^+ cells expressing the indicated molecules, expressed as % (±SEM) of total $CD34^+$ cells

Table 2 – Summary of fibrocyte subtypes (by immunocytofluorescence) in circulation of the three strains of mice

	Subtypes of fibrocytes in circulation 2-3 days post-injury (% of $CD34^+$ cells)			Phenotype (Day 28)	Administration of anti-hTFPI antibody
Strain	$CD34^+$ collagen-1^+	$CD34^+$ collagen-1^+ α-SMA^+	$CD34^+$ collagen-1^+ α -SMA^+, $CD31^+$		
WT	46%	7%	3%	IH, luminal fibrocytes	No effect
CD31-TFPI-Tg	44%	6%	3%	No IH, luminal fibrocytes	IH, but no change in circulating fibrocyte subsets
α-TFPI-Tg	35%	0.01%	0%	No IH, luminal EC	IH, circulating fibrocyte subsets as in WT, luminal fibrocytes

IH intimal hyperplasia; EC Endothelial cells;

Table shows proportion of $CD34^+$ cells expressing the indicated molecules, expressed as % (±SEM) of total $CD34^+$ cells

Table 3: Double stain immunocytofluorescence analysis of CD34$^+$ α-SMA$^+$ cells in α-TFPI-Tg mice

	CD34$^+$α-SMA$^+$cells – Day 3			
	% (±SEM) of CD34$^+$α-SMA$^+$cells expressing these ligands			
	α-TFPI-Tg	p value vs WT (vs CD31-TFPI-Tg)*	α-TFPI-Tg +anti-hTFPI	p value†
CD90	100	-	100	-
Collagen-1	3.7 (±3.7)	0.00009 (0.002)	85.7 (±1.4)	0.00003
Fibronectin	2.8 (±2)	0.009 (0.001)	58.1 (±8.3)	0.003
Flk-1	0	0.01 (0.02)	ND	-
CD31	0	0.01 (0.02)	50 (±12.4)	0.02
CD45	12.2 (±6.2)	0.02 (0.03)	41.3 (±4)	0.02
F4/80	10.2 (±6.5)	0.002 (0.04)	50.3 (±11)	0.04
Ly6-C	16.9 (±2.6)	0.004 (0.0005)	53.1 (±1.6)	0.0002
CD11b	21.7 (±6)	0.01 (0.007)	53 (±10)	0.05
CD115	9.3 (±4.7)	0.03 (0.01)	45 (±6.4)	0.01
TIE-2	31.5 (±11)	NS (NS)	69.9 (±6.3)	0.04
CD140b	35.4 (±7.5)	0.009 (0.02)	4.8 (±4.8)	0.03
NG2	66.2 (±4.4)	0.0001 (0.0007)	10 (±6.5)	0.002
Angiopoietin-1	96.3 (±3.7)	0.0003 (0.009)	48.7 (±1.3)	0.003
Angiopoietin-2	4.2 (±4)	0.003 (0.02)	50.9 (±15.2)	0.04
CXCL12	9(±5.9)	0.0002 (0.02)	62.5(±12.5)	0.02
CXCR4	16.1 (±12.2)	0.005 (NS)	71.9 (±1.7)	0.01

* see data in table 1

† α-TFPI-Tg + anti-hTFPI vs. α-TFPI-Tg

Table shows proportion of CD34$^+$ α-SMA$^+$ cells expressing the indicated molecules, expressed as % (±SEM) of total CD34$^+$ cells

Figure Legends

Figure 1- Recruitment to intima of WT and CD31-Tg.

3-colour confocal overlay images of consecutive frozen sections from post-injury carotid arteries. Day 0 = 20 hours post-injury. All sections stained with DAPI (blue): (red); anti-α-SMA,-CD31, -TF or -E-selectin as indicated and (green); anti-CD31, -34, -45,-collagen-1, hTFPI or fibronection as indicated. Yellow indicates co-localisation. A; WT C; CD31-TFPI-Tg. B & D; show enlarged images from the boxed areas in A & C. Images from a single artery representative of n=6 animals from each strain. Experiment performed twice.

Figure 2 – Phenotype of CD31-TFPI-Tg mice

A&B: Flow cytometry of: A; whole blood mononuclear cells, gated on CD34 and CD45 expression; B; purified $CD34^+$ cells. Open profile hTFPI, closed profile isotype control. Flow cytometry repeated x3.

C-E: 3-colour immunocytofluorescence of fixed/permeabilised purified $CD34^+$ cells stained with DAPI (blue) and hTFPI (green) with (red) either CD31 (C&D) or α-SMA (E). In all, the right panel = overlay image. In D&E, the anti-hTFPI was applied before fixation.

F: Three colour IF of vessels from CD31-TFPI-Tg mice day 28 post-injury. Stained with DAPI (blue), anti-α-SMA (red) & anti-CD31 (green). Yellow = co-localisation. Mice received anti-hTFPI Ab on day of injury. Scale bars 100μm.

G: Morphometric analysis of injured vessels from experiments using CD31-TFPI-Tg mice. Graphs show neointimal area + SEM (left) and neointima:media ratios + SEM (right) of vessels 28 days post-injury. Animals given 7.5 $x10^5$ $CD34^+$ cells on the day

of injury. Data derived from three random sections from each of 5 different vessels. Derived from 2 independent experiments.

Figure 3 - Recruitment of cells to intima of α-TFPI-Tg arteries

A&B: 3-colour confocal overlay images of consecutive frozen sections from carotid arteries from α-TFPI-Tg mice. Day 0 = 20 hours post-injury. A: all sections stained with DAPI (blue) and (red); anti-α-SMA, -CD31, -TF or -E-selectin as indicated and (green); anti-CD31, -CD34, -CD45 or -collagen-1 as indicated. B shows enlarged images from the boxed area in A. Yellow indicates co-localisation. White arrows in images in B indicate the same $CD31^+$ cells. Images from a single artery representative of n=6 animals. Experiment performed twice.

C&D Three colour immunohistological analysis of consecutive frozen sections from day 28 carotid arteries from α-TFPI-Tg mice that received isotype control (C) or anti-hTFPI Ab (D) on day of injury. All sections stained with DAPI (blue) and anti-α-SMA (red) and either (green) anti-TF (left panel), anti-CD31 (middle panel) or anti-E-selectin (right panel) as indicated. Yellow indicates co-localisation.

E&F: 2-colour immunohistological analysis from WT mice 7 days post-injury, each given 7.5 $x10^5$ $CD34^+$ cells from α-TFPI-Tg mice on day of injury. Sections with (red); anti-α-SMA, -vWF, -CD45 or –CD34 as indicated and (green); anti-hTFPI; F shows enlarged images from the boxed areas in E. White arrows in E indicate the same area of lumen in consecutive sections. Images from a single artery representative of n=6 animals. Experiment performed twice.

G: Three colour immunocytofluorescence images of $CD34^+$ cells from α-TFPI-Tg mice, 2 days posy-injury. All mice received anti-hTFPI antibody on day of injury. Right panel = overlay images. Arrows show double-positive cells.

Figure 4: Phenotype of CD34+ cells from α-TFPI-Tg

A: Flow cytometry of whole blood mononuclear cells from α-TFPI-Tg mice, showing hTFPI fusion protein by subsets of cells analysed by CD34 expression.

B: Flow cytometry of purified $CD34^+$ cells. Open profile; hTFPI. Closed profile; isotype control. Flow cytometry repeated x3

C-H: Representative three colour immunocytofluorescence images from α-TFPI-Tg mice. Blue = DAPI. Left panel (red) stained with anti-α-SMA, -CD31 or –hTFPI as indicated; Middle panel (green) stained with anti-CD31, hTFPI, -CD45, or –NG2 or collagen-1 as indicated. Right panel = overlay images. Arrows show double-positive cells.

I: Real time RT-PCR analysis of collagen-1 expression in CD34-negative (blue bars) and CD34+ fractions (red). Collagen-1 expression is normalised to housekeeping TBP RNA.

J: Relationship between % of the $CD34^+\alpha\text{-}SMA^+$ cells expressing collagen-1 by immunocytofluorescence (abscissa) and RT-PCR results in I.

K: Analysis of phenotype of WT or PAR $^{-/-}$ $CD34^+$ cells 3 days post injury, determined by immunocytofluorescence. White = total $\alpha\text{-}SMA^+$ cells, Black = $\alpha\text{-}SMA^+CD31^+$ cells; Grey = total $CD31^+$ cells.

L-P: $CD34^+$ cells were incubated in medium with thrombin for 1 or 5 (default) days. White bars = $\alpha\text{-}SMA^+CD31^-$ cells, Black = $\alpha\text{-}SMA^+CD31^+$; Grey = $\alpha\text{-}SMA^-CD31^+$ cells. In O, the $CD34^+$ were depleted of $hTFPI^+$ cells prior to incubation. Data derived

from counting at least 100 stained cells from each of 5 different animals. Experiments performed twice.

Figure 1

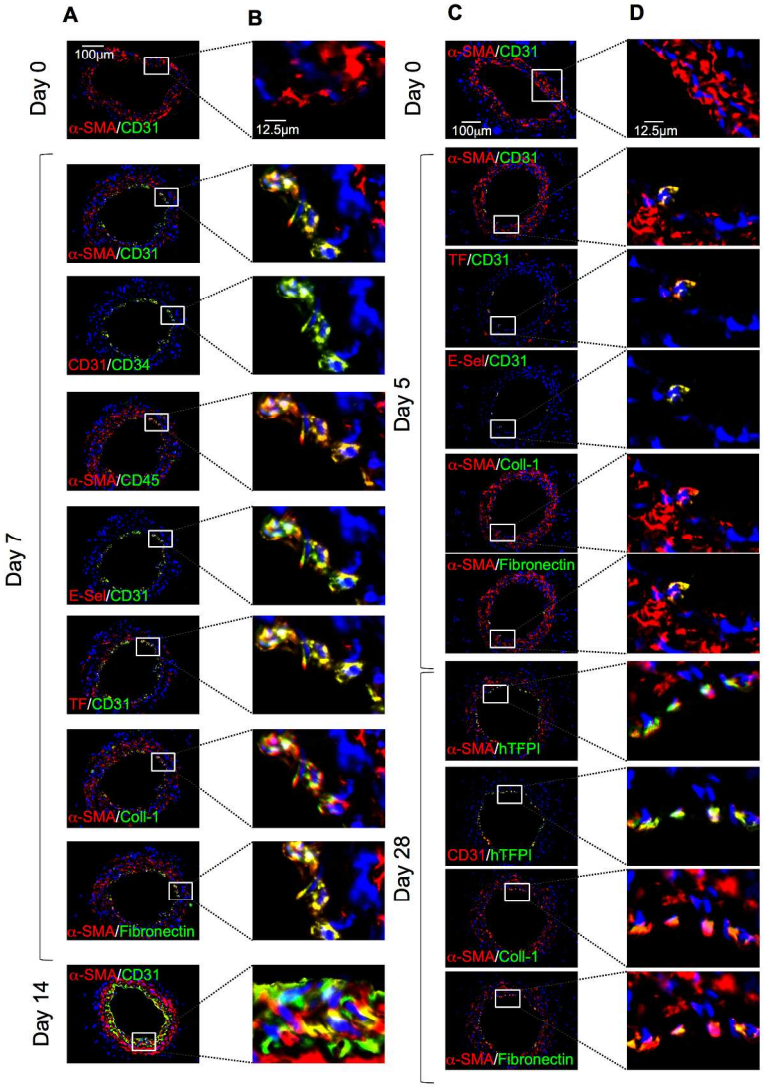

190x279mm (300 x 300 DPI)

Figure 2

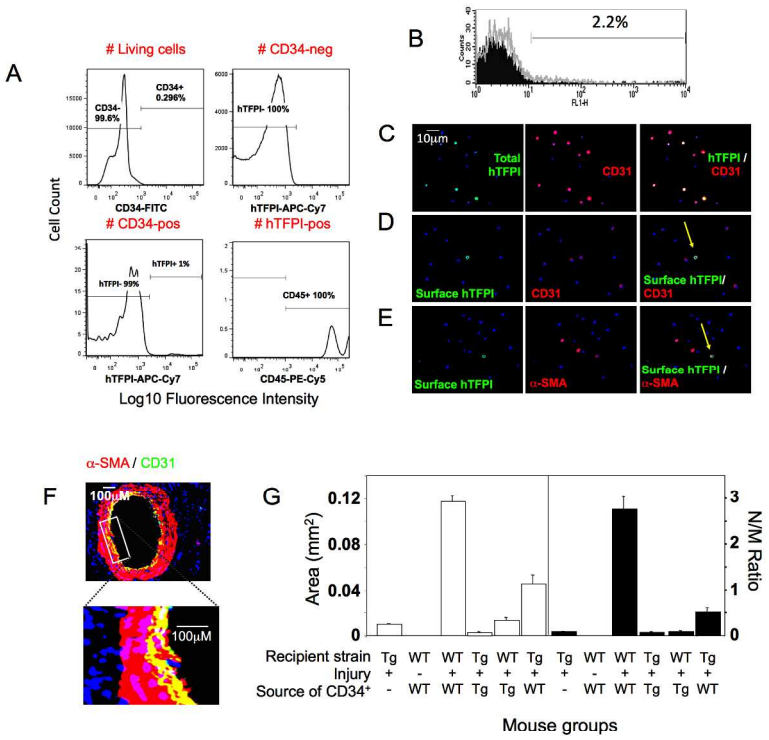

190x279mm (300 x 300 DPI)

Figure 3

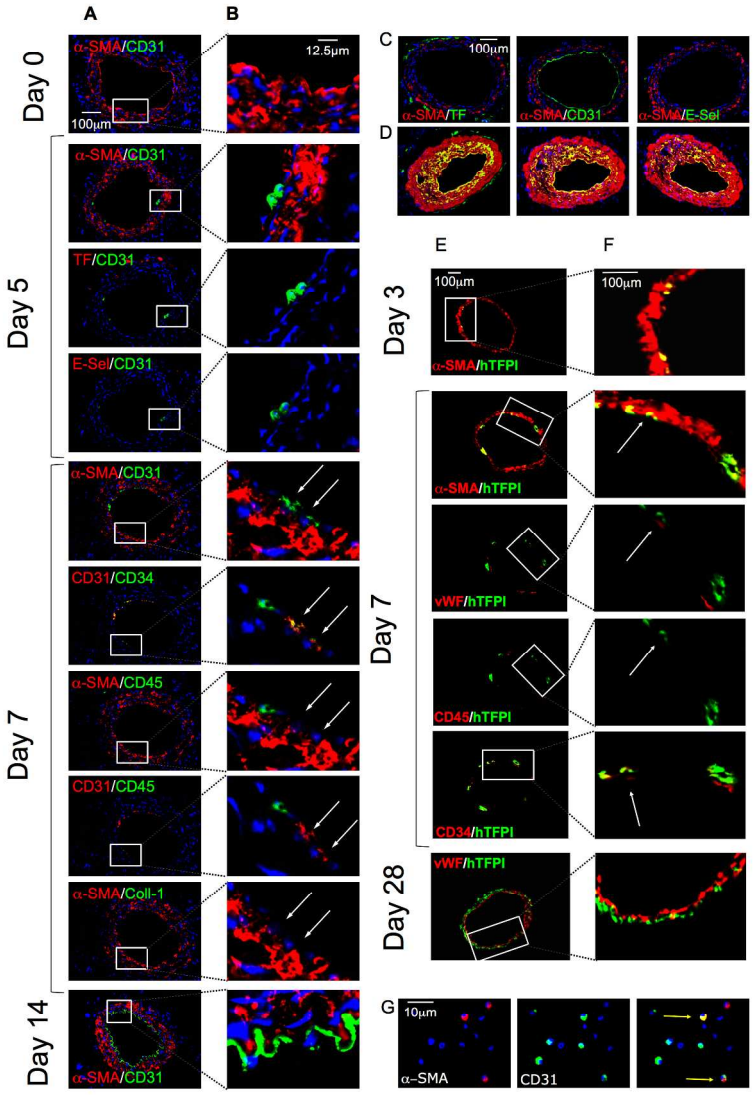

190x279mm (300 x 300 DPI)

Figure 4

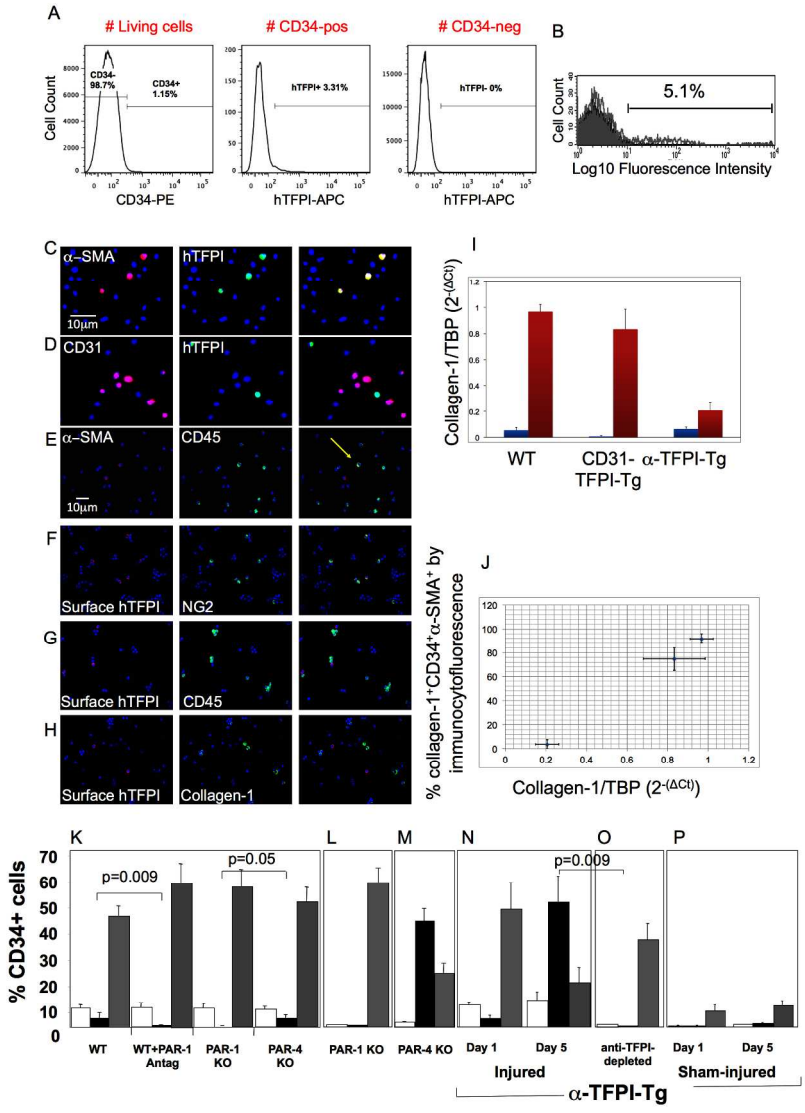

190x279mm (300 x 300 DPI)

Online Supplementary Material

Fibrocytes mediate intimal hyperplasia post-vascular injury and are regulated by two tissue factor-dependent mechanisms.

Chen: intimal hyperplasia, TF& fibrocytes.

D. Chen,

L. Ma,

E-L Tham,

S. Maresh,

R. I. Lechler,

J. H. McVey,

A. Dorling.

Medical Research Council (MRC) Centre for Transplantation, King's College London, King's Health Partners, Guy's Hospital, Great Maze Pond, London UK SE1 9RT

Corresponding Author: Prof. Anthony Dorling, MRC Centre for Transplantation, King's College London, Guy's Hospital, London, UK SE1 9RT

Tel +44 (0)20 7188 5880 Fax +44 (0)20 7188 5660

Email; anthony.dorling@kcl.ac.uk

Detailed Materials and Methods

Animals and experimental models. C56BL/6 (WT) mice (Harlan Olac Ltd Bicester, UK), heterozygous CD31-TFPI-Tg [1], α-TFPI-Tg [2], homozygous PAR-$1^{-/-}$ (derived from strain B6.129S4-F2rtm1Ajc/J) and PAR-$4^{-/-}$ mice (derived from strain B6.129S4-F2rl3tm1.1Cgh) [3], were bred and maintained at King's College London. All genetically modified animals have been maintained for more than 10 generations on a WT background. All procedures were approved by the UK Home Office.

Wire-induced endoluminal carotid artery injury: This was performed as previously described [2, 4]. Briefly, a 100μm diameter wire was introduced and withdrawn three times into the common carotid via the external carotid artery before the external carotid artery was tied off. After confirming restoration of normal blood flow through the common carotid, the skin was closed and animals were allowed to recover from anaesthesia. Some mice received anti-human TFPI (Enzyme Research Laboratories, Swansea, UK) or Isotype control (both 80 ng/g in 50 μl saline) by tail vein immediately after injury. Others received 10μg/kg Mercaptopropionyl-Phe-Cha-Arg-Lys-Pro-Asn-Asp-Lys-NH2 (PAR-1 antagonist), 200 ng of Angiopoietin-2 (R&D Systems,Oxon, UK) or 0.1% bovine serum albumin (vehicle – Sigma, Dorset UK) in 50 μl saline by tail vein injection once a day for 2 days.

Morphometric analysis and immunohistology. Arterial sections were prepared and examined as previously described [2, 4]. Briefly, vessels were isolated and embedded in OCT (VWR International, Dorset, UK) by freezing with dry ice, sectioned at 4-5μm thickness and fixed in methanol at –20˚C. For

analysis of intimal and medial areas, sections were stained using the Accustain™ Elastin Stain kit (Sigma) and examined using LUCIA Imaging Software (Lucia Software, Exeter, UK) associated with a Leitz microscope (Leitz, Wetzlar, Germany) equipped with a Nikon digital camera DXM 1200F (Nikon Corporation, Japan) and objectives EF x10/0.25 and EF x25/0.50. At least three random sections were examined from each of six wire-injured arteries. For immunofluorescence (IF) analysis, consecutive sections were double-stained with appropriate combinations of mouse anti-human α-SMA conjugated with Cy3 (Sigma-Aldrich, MO, USA), human TFPI (American Dignostica, CT, USA); rabbit anti-mouse CD31(Reprokine, NY USA), CD45, E-selectin, α-SMA, fibronectin, collagen 1 (Abcam, Cambridge, UK), TF [5] human von Willebrand Factor (vWF) (Dako, Cambridge, UK); Goat anti-NG2 (Abcam) or rat anti-mouse CD34, CD31 (BD Biosciences, Oxford, UK) and CD45 (Abcam). The following anti-IgG FITC-conjugated antibodies were used: sheep anti-mouse, goat anti-rat, goat anti-rabbit and rabbit anti-goat (Sigma). All stained sections were mounted in Vectashield with DAPI (Vector Laboratories Inc, CA USA). Sections were directly captured and examined by a Leica DMIRBE confocal microscope (Leica, Wetzlar, Germany) equipped with Leica digital camera AG and a confocal laser scanning system with excitation lines at 405, 488, 543, and 560 nm at magnifications 10x/0.40CS and 20x/0.70IMM (Leica, Planapo, Wetzlar, Germany). Images were processed using Leica-TCS-NT software associated with the Leica confocal microscope. Other sections were captured by IF microscope (Olympus BX51) and analysed with Micro-Manager 1.3 together with Image J software (BioArts, Maryland, USA). All IF was performed at 22^{o} C. For estimations of

cell density, average counts were derived from examination of at least six random sections from each artery.

CD34$^+$ experiments. Murine peripheral blood was collected into 1mM EDTA or 3.2% sodium citrate and diluted with 2% FCS-PBS. Pelleted cells were re-suspended in ACK buffer and left at room temperature for 25 minutes, before washing to remove platelets.

For flow cytometric analysis, cells were incubated with anti-mouse CD16/CD32 FcR block (eBioscience, Hatfield UK) before staining with combinations of LIVE/DEAD(R) Fixable Aqua Dead Cell Stain (Invitrogen, Paisley, UK), rat anti-mouse CD34 PE (BD Biosciences), CD45 eFluor® 450 (eBioscience) and mouse anti-human TFPI followed by APC-conjugated rat anti-mouse IgG1 (BD Bioscience). Appropriate istotype controls were used to establish gating strategy. Samples were run on a BD Biosciences LSR Fortessa and data analysed using FlowJo software.

Purified CD34$^+$ cells were isolated using magnetic beads (Miltentyi Biotech, Surrey UK) as previously described [2, 4] and had an average purity of 95%.

For immunocytofluorescence (ICF), cells were fixed with cold methanol for 10 minutes on polylysine-coated slides (VWR International, Leuven, Belgium) before staining with combinations of mouse anti–human α-SMA conjugated with Cy3 (Sigma-Aldrich); rat anti-mouse Flk-1, Ly6-C, CD11b or CD115 (eBioscience), CD140b (Biolegend, Cambridge, UK), CD31 (BD Biosciences), CD45, F4/80, CD90, α–SMA (Abcam); mouse anti-human TFPI (American Diagnostia); Goat anti-PAR-1 (Santa Cruz Biotechnology, CA, USA), NG2 (Abcam); rabbit anti– mouse TF [5], PAR-4 (AutogenBioclear, Wiltshire,

United Kingdom), E-selectin, Angiopoietin-1, Angiopoietin-2, TIE-2, fibronectin or collagen-1 (Abcam). Second layer staining was with a goat anti-rat IgG-FITC, goat anti-rabbit IgG-FITC or rabbit anti-goat IgG-FITC (all from Sigma-Aldrich). Some cells were triple-stained with mouse anti–human α-SMA conjugated with Cy3, rabbit anti-CD31 (Reprokine) and rat anti-mouse CD45 (Abcam) followed by FITC-conjugated anti-rabbit IgG and AMCA-conjugated donkey anti-rat IgG (Millipore, MA, USA). To determine cell surface expression of the hTFPI fusion protein, CD34+ cells were directly stained with rabbit anti-human TFPI (American Dignostica) before fixation with cold methanol. TRITC- conjugated goat anti-rabbit IgG (Sigma) was used as secondary. Labelled cells were captured at the laser lines 405, 488 and 543 nm on an IF microscope equipped with objectives UPLANFL 20X/NA0.50 AND 40X/NA 0.75 (Olympus BX51) and a charge-coupled device (CCD) camera (Q Imaging, Surrey, BC Canada) and analyzed as above. To determine subpopulation densities, a total of 300 cells were counted at ×200 magnification from at least 3 random fields from 3 different wells.

For functional experiments, $CD34^+$ cells were purified from mice 2-4 days after injury and incubated in vitro with up to 50 nM thrombin (Enzyme Research Laboratories) in Iscove modified Dulbecco medium (Sigma-Aldrich) supplemented with 2% fetal bovine serum (StemCell Technology, Grenoble, France) for 0, 1 or 5 days. For adoptive transfer experiments, $1x10^7$ $CD34^+$ cells were injected via a tail vein.

For analysis by RT-PCR, cells were stored in RNA*later* (Ambion) at -20°C until use. RNA was separated from these cells using the RNAqueous-4PCR kit (Ambion), according to manufacturer's protocol and RNA concentration

and quality was determined using a Nanophotometer (Implen). cDNA was made from the extracted RNA using the SuperScript VILO cDNA Synthesis Kit (Invitrogen). cDNA systhesis was run on a S100 Thermal Cycler (Bio Rad). cDNA is then stored in -20°C until use. RT-PCR was performed using Express qPCR SuperMix (with premixed ROX) (Invitrogen) and using TaqMan Gene Expression Assays (Applied Biosystems) for Collagen 1, Assay ID: Mm00801666_g1 (Applied Biosystems) and TBP, Assay ID: Assay ID: Mm00435546_m1(Applied Biosystems). All RT-PCR were run on a C100 Thermocycler with a CFX-96 Real-Time PCR Detection Optical Reaction Module (Bio Rad).

Statistical analysis. Data are presented as means ±SEM. Significance of the difference between 2 groups was determined by unpaired Student *t* or log rank test. Values of $P<0.05$ were considered statistically significant.

References

1 Chen D, Giannopoulos K, Shiels PG, Webster Z, McVey JH, Kemball-Cook G, Tuddenham E, Moore M, Lechler R, Dorling A. Inhibition of intravascular thrombosis in murine endotoxemia by targeted expression of hirudin and tissue factor pathway inhibitor analogs to activated endothelium. *Blood*. 2004; **104**: 1344-9. 10.1182/blood-2003-12-4365.

2 Chen D, Weber M, Shiels PG, Dong R, Webster Z, McVey JH, Kemball-Cook G, Tuddenham EG, Lechler RI, Dorling A. Postinjury vascular intimal hyperplasia in mice is completely inhibited by CD34+ bone marrow-derived progenitor cells expressing membrane-tethered anticoagulant fusion proteins. *J Thromb Haemost*. 2006; **4**: 2191-8. 10.1111/j.1538-7836.2006.02100.x.

3 Connolly AJ, Ishihara H, Kahn ML, Farese RV, Jr., Coughlin SR. Role of the thrombin receptor in development and evidence for a second receptor. *Nature*. 1996; **381**: 516-9. 10.1038/381516a0.

4 Chen D, Abrahams JM, Smith LM, McVey JH, Lechler RI, Dorling A. Regenerative repair after endoluminal injury in mice with specific antagonism of protease activated receptors on CD34+ vascular progenitors. *Blood*. 2008; **111**: 4155-64. 10.1182/blood-2007-10-120295.

5 Mumford AD, Chen D, Dorling A, Kemball-Cook G, McVey JH. Generation of a polyclonal rabbit anti-mouse tissue factor antibody by nucleic acid immunisation. *Thromb Haemost*. 2005; **93**: 160-4. 10.1267/THRO05010160.

Suppl. Table 1: Single stain immunocytofluorescence analysis of CD34$^+$ cells

	CD34$^+$ cells – Isolated day 3 post-injury				
	% (±SEM) of CD34$^+$ cells expressing these ligands				
	WT	CD31-TFPI-Tg	p value	CD31-TFPI-Tg + anti-hTFPI	p value†
TF	67.7 (±6.4)	51 (±6.8)	NS	69 (±11.6)	NS
CD45	48 (±3.5)	42 (±5.5)	NS	ND	-
F4/80	34.3 (±3.9)	32.3 (±7.9)	NS	ND	-
Ly6-C	33 (±3.2)	33.7 (±4.2)	NS	ND	-
CD11b	34.7 (±5.8)	33.3 (±6.7)	NS	ND	-
CD115	34 (±5)	33.7 (±4.3)	NS	ND	-
Collagen 1	45.7 (±5)	43.7 (±5)	NS	ND	-
CD90	29 (±4.6)	31 (±3.5)	NS	ND	-
CD140b	33 (±7)	26.7 (±6)	NS	ND	-
α-SMA	8 (±1.7)	8 (±1.2)	NS	8 (±1.3)	NS
Fibronectin	7.3 (±1.2)	5.7 (±0.7)	NS	ND	-
FLK-1	87.7 (±6)	88.7 (±6)	NS	68 (±3.6)	NS
CD31	54.3 (±4.6)	52.6 (±3.6)	NS	54.2 (±2.9)	NS
E-sel	44 (±5)	20.3 (±5.2)	0.03	39.3 (±7.1)	NS
TIE-2	66.3 (±8.7)	60 (±2.5)	NS	67.3 (±7.9)	NS
NG2	0.3 (±0.3)	1.3 (±0.7)	NS	ND	-

† CD31-TFPI-Tg + anti-hTFPI vs. CD31-TFPI-Tg

Table shows proportion of CD34$^+$ cells expressing the indicated molecules, expressed as % (±SEM) of total CD34$^+$ cells

Suppl Table 2 – Circulating CD34$^+$ cells post-allogeneic transplantation

	CD34$^+$α-SMA$^+$cells – Isolated day 7 post-transplantation		
	% (±SEM) of CD34$^+$α-SMA$^+$cells expressing these ligands		
	WT	α-TFPI-Tg	P value
Collagen-1	86.4 (±6.9)	1.9 (±1.9)	0.0003
NG2	0	76.1 (±5.8)	0.0002

Table shows proportion of CD34$^+$ α-SMA$^+$ cells expressing the indicated molecules, expressed as % (±SEM) of total CD34$^+$ cells

Suppl. Table 3: Single stain immunocytofluorescence analysis of CD34$^+$ cells

	CD34$^+$ cells – Isolated day 3 post-injury			
	% (±SEM) of CD34$^+$ cells expressing these ligands			
	α-TFPI-Tg	p value vs. WT (vs. CD31-TFPI-Tg)*	α-TFPI-Tg +anti-hTFPI	p value†
TF	42 (±8.3)	NS (NS)	74.7 (±7.9)	0.05
CD45	38 (±4.4)	NS (NS)	50 (±6.4)	NS
F4/80	30.3 (±5.6)	NS (NS)	38.7 (±3.3)	NS
Ly6-C	31 (±2.5)	NS (NS)	40 (±7)	NS
CD11b	31.7 (±5)	NS (NS)	40.7 (±5.2)	NS
CD115	31.7 (±5)	NS (NS)	38.3 (±4.7)	NS
Collagen-1	32.3 (±5.5)	NS (NS)	44 (±7.5)	NS
CD90	29 (±3.2)	NS (NS)	29.7 (±1.5)	NS
CD140b	25 (±4.4)	NS (NS)	26 (±4)	NS

α-SMA	8.3 (±0.8)	NS (NS)	8 (±1)	NS
Fibronectin	0.7 (±0.3)	0.06 (0.003)	6 (±1.7)	0.04
FLK-1	87 (±5)	NS (NS)	ND	-
CD31	54.9 (±4.8)	NS (NS)	54.9 (±3.9)	NS
E-sel	5 (±2)	0.002 (0.05)	36.7 (±7.5)	0.02
TIE-2	32.7 (8.6)	0.05 (0.04)	67.3 (±7.4)	0.04
NG2	7.7 (±1.8)	0.02 (0.03)	1.3 (±0.7)	0.03

* see data in Suppl. table 1

† α-TFPI-Tg + anti-hTFPI vs. α-TFPI-Tg

Table shows proportion of $CD34^+$ cells expressing the indicated molecules, expressed as % (±SEM) of total $CD34^+$ cells

Suppl. Table 4: Double stain ICF analysis of $CD34^+$ cells

	$CD34^+\alpha\text{-}SMA^+$cells – Isolated day 3 post-injury			
	%(±SEM) of $CD34^+\alpha\text{-}SMA^+$cells expressing these ligands			
	PAR-1 KO	p value vs. WT (vs. α-Tg)*	PAR-4 KO	p value vs. PAR-1 KO
Collagen 1	3.7 (±3.7)	0.0001 (NS)	60.6 (±10.6)	0.007
Fibronectin	4.2 (±4.2)	0.001 (NS)	55.3 (±1.1)	0.0003
CD140b	20.3 (±1)	0.0004 (NS)	3.3 (±3.3)	0.008
NG2	67.1 (±6.8)	0.0006 (NS)	9.4 (±5.8)	0.003

* see data in Table 3 main article

Table shows proportion of $CD34^+$ $\alpha\text{-}SMA^+$ cells expressing the indicated molecules, expressed as % (±SEM) of total $CD34^+$ cells

Suppl. Table 5: Double stain ICF analysis of CD34$^+$α-SMA$^+$ cells after incubation with thrombin

	CD34$^+$cells after thrombin incubation				
	% (±SEM) of total CD34$^+$cells expressing these ligands				
Mouse strain / Cell phenotype	Day 0	Day 1	p value	Day 5	p value (vs. day 0)
PAR-1 $^{-/-}$					
CD31$^+$ α-SMA$^+$	0.3 (0.3)	ND*	-	1.3 (±0.3)	- (NS)
PAR-4 $^{-/-}$					
CD31$^+$ α-SMA$^+$	3.7 (±1.2)	ND	-	42.7 (±5.8)	- (0.02)
α-TFPI-Tg					
Total α-SMA$^+$	8.4 (±1.1)	13.3 (±1)	0.003	57.3 (±3.6)	1x10^{-14} (3x10^{-13})
Total CD45$^+$	38.4 (±1.9)	58.4 (±2.1)	3.3x10^{-6}	85.4 (±2)	2x10^{-8} (3x10^{-13})
CD45$^+$ α-SMA$^+$	1 (±0.6)	ND	-	37.33 (±4.8)	- (0.002)
Flk-1$^+$ α-SMA$^+$	0	4.7 (±1.7)	0.05	51.3 (±10.8)	0.01 (0.009)
CD31$^+$ α-SMA$^+$	0	3.3 (±1.2)	0.05	49.3 (±10.5)	0.01 (0.009)
hTFPI$^+$ α-SMA$^+$	8.3 (±3)	12 (±3.2)	NS	60 (±15)	0.04 (0.03)
Collagen-1$^+$ α-SMA$^+$	0.3 (±0.3)	ND	-	53 (±5.3)	- (0.0006)
Fibronectin+ α-SMA$^+$	0.3 (±0.3)	ND	-	58 (±5.5)	- (0.0004)
CD140b+ α-SMA$^+$	3.3 (±0.9)	ND	-	0.3 (±0.3)	- (0.03)
NG2+ α-SMA$^+$	7.3 (±1.9)	ND	-	0.6 (±0.3)	- (0.02)
Angio-1+ α-SMA$^+$	6.7 (±2.7)	2.7 (±1.2)	NS	2 (±0.6)	NS (NS)
Angio-2+ α-SMA$^+$	0	6.7 (±2.3)	0.05	54.3 (±6.4)	0.002 (0.001)

*ND=not done

Table shows proportion of CD34$^+$ cells expressing the indicated molecules, expressed as % (±SEM) of total CD34$^+$ cells. The cells were isolated day 3 post-injury from the mouse strains indicated, and incubated with thrombin for 0, 1 or 5 days, as indicated.